Tribological analysis of a 3D-printed internal triangular flip ABS pin during running-in stage

Mohamad Nordin Mohamad Norani [1], Muhammad Ilman Hakimi Chua Abdullah [2,3*], Mohd Fadzli Bin Abdollah [1,3], Hilmi Amiruddin [1,3], Faiz Redza Ramli [1,3], Noreffendy Tamaldin [1,3]

[1] Fakulti Kejuruteraan Mekanikal, Universiti Teknikal Malaysia Melaka, Hang Tuah Jaya, 76100 Durian Tunggal, Melaka, MALAYSIA.
[2] Fakulti Teknologi Kejuruteraan Mekanikal & Pembuatan, Universiti Teknikal Malaysia Melaka, Hang Tuah Jaya, 76100 Durian Tunggal, Melaka, MALAYSIA.
[3] Centre for Advanced Research on Energy, Universiti Teknikal Malaysia Melaka, Hang Tuah Jaya, 76100 Durian Tunggal, Melaka, MALAYSIA.
*Corresponding author: ilmanhakimi@utem.edu.my

KEYWORDS	ABSTRACT
3D printing Tribology ABS Running-in COF	The objective of this study was to investigate the correlation between the coefficient of friction (COF) and the running-in distance as well as the wear properties of acrylonitrile butadiene styrene (ABS) polymer. This was achieved by comparing a 3D-printed internal triangular flip ABS pin with a 3D-printed solid ABS pin under varying loads and sliding speeds. The ABS pin that was investigated was modified into a triangular flip internal structure and manufactured via 3D printing through fused filament fabrication (FFF). The experiment was conducted under dry conditions using a pin-on-disc tribometer. At a load of 58.68 N and sliding speed of 600 rpm, the running-in distance of 145.16 m showed that the triangular flip ABS pin produced a lower steady-state COF (0.305) compared to the solid ABS pin. The triangular flip ABS pin exhibited the effects of an early contact microstructure as well as changes in the surface area composition that resulted in a low maximum stress, thereby decreasing the COF. A morphological analysis using scanning electron microscopy (SEM) revealed that delamination and abrasion were the main mechanisms of wear.

1.0   INTRODUCTION

Polymers are being used in various applications due to their wide range of properties. In the automobile industry, acrylonitrile butadiene styrene (ABS) polymer is mainly used in the manufacture of radiator grills, panels, door trims, headlight housings, consoles, and interior trims. ABS is also used in the production of devices such as radios, computers, telephone handsets, and televisions. Running-in distance is defined as the minimum distance needed to reach a steady state, which is often occurs at initial surface process, when sliding or rolling is established between the contact surfaces of two solid bodies. The wear inflicted on the contact surfaces will lead to fatigue, erosion, and abrasion (Zmitrowicz, 2006). Failure to take into account the tribological interactions coupled with a lack of information have contributed significantly to the poor performance of high-end machine parts and a waste of resources. Besides that, a better understanding of the friction distance and wear will help to enhance the wear rate, durability and stability of a machine. The sliding contact between metallic parts and polymers is significantly difficult to understand compared to the sliding contact between metallic parts and metals (Brostow et al., 2006; Bakar et al., 2020).

Frictional and wear behaviours, likewise called a break-in or running-in map, are difficult to replicate, even under identical test conditions, and hard to characterise. Whereas under dry and unlubricated conditions, they are expected to provide the most clearly definable microstructural effects on initial friction and wear transients. Moreover, a break-in map indicates the power consumption, also known as the sliding resistance, within a given system. The stability of a whole break-in combination curve (oxide, plastic deformation and abrasive debris) can be determined by three factors: (1) the stability of external sliding settings such as the load, temperature and velocity; (2) the stability of each contributing process and its subsequent influence on the net friction; and (3) its effect on the material (e.g. wearing through coatings and time-dependent changes to the structure or composition of the material) (Blau., 1981).

Fused filament fabrication (FFF) is an additive manufacturing (AM) process that is normally used in 3D printing applications. It is a method of manufacturing via extrusion, where the selected material is injected through a nozzle. 3D-printed parts are currently being used as prototypes for visual aids, presentation models, or for fittings and assemblies. FFF is being used in manufacturing fields for the rapid production of goods (Samira et al., 2018; Liu et al., 2019; Sabahi et al., 2020; Jasiuk et al., 2018). However, its use in diverse applications calls for the materials to be thoroughly tested to determine their suitability and stability when subjected to mechanical loading. Therefore, the mechanical properties of FFF-manufactured parts necessitate keen study and research.

Hanon et al. (2020) examined the impact of a 3D-printed structure on the tribological properties of polymers. The test pieces, Polylactide acid (PLA), high tensile/high temperature PLA (HT-PLA) and Polyethylene terephthalate-glycol (PETG), were fabricated using FDM at different print orientations horizontally (X) and vertically (Z). They found that the maximum dynamic COF at the Z-oriented PETG polymer was on average about 0.44. In contrast, the HT-PLA polymer printed in the X orientation showed a 30% difference in comparison with the greatest value. Also, different orientations in the 3D printing process also resulted in variations in the wear depth, where the highest wear depth was 0.594 mm^3 at the Z-oriented HT-PLA, and the lowest wear depth was 0.1365 mm^3 at the X-oriented HT-PLA. These findings suggest that printing should be carried out in the horizontal orientation (X) to reduce friction and wear.

Correspondingly, Hanon et al. (2020) studied the effects of the print orientation and the presence of bronze on the tribological and mechanical properties of 3D-printed bronze/PLA

composites. This paper explored the impact of the process settings (orientation) and the presence of bronze on the mechanical and tribological properties (in terms of wear and friction) of 3D-printed bronze/PLA composites. It was learned that the FDM 3D printer with an average accuracy of 98.78% and an on-edge print orientation gave the highest tensile stress and break point elongation of 28 MPa and 2.5-3%, respectively compared to flat and upright specimens. In terms of the tribological test, the horizontal orientation at an angle of 45° produced the lowest COF due to the difference in surface roughness. However, in the wear depth analysis, it was shown that the vertical orientation produced the least wear, since the contact area of the sliding counterparts was smaller compared to the samples with other print orientations.

Norani et al. (2020) analysed the tribological properties of 3D-printed ABS by studying the correlation between nozzle temperature, layer height and printing pattern as the control variables to optimise the coefficient of friction (COF) and wear rate using RSM. The results revealed that the layer height had the most significant impact compared to the nozzle temperature and printing pattern. It was then suggested that the optimal COF and wear rate for 3D-printed ABS are a layer height of 0.10 mm, a triangular pattern, and a nozzle temperature of 234°C, with a percentage error of 2.16% for the COF and 6.78% for the wear rate.

Hanon et al. (2019) analysed the tribological properties of two ABS polymer samples. One sample was manufactured via extrusion fabrication (3D printing), while the other was manufactured through subtractive manufacturing (lathe turning). The wear levels of the samples were taken into consideration during the study. The study concluded that the dynamic friction of 0.1 of the lathe-turned machined sample was better than that of the 3D-printed sample. The adhesion wear was stronger in the lathe-turned machined sample in comparison to the 3D-printed sample due to the lower difference in the surface pressure. The surface of the 3D-printed sample was rough, while the lathe-turned machined sample was smooth.

In addition, the influence of the 3D printing parameters on the tribological characteristics is also important. Nor et al. (2018) studied the effects of the FFF process by using the Taguchi method. They examined the tensile stress of the ABS material and carbon fibre-reinforced ABS (CFRABS), with the layer thickness and filled angle as the input variables. The layer thickness had a major impact of 86.956% on the tensile stress of the ABS material, while the filled angle had an effect of 75.14% on the tensile stress of the CFRABS material. This enhanced the toughness, impact strength and rigidity of the material.

With regard to the influence of normal loads on the COF and wear rate of different polymers and composite materials, Nuruzzaman et al. (2011) concluded that the COF and wear rate vary from material to material. Franklin (2001) reported that the wear behaviour of polymers under dry reciprocating sliding conditions does not always follow the generally accepted engineering rule of 'the higher the sliding speed, the higher the wear rate'. It is, therefore, significantly difficult to understand the interaction between sliding metallic parts and polymers compared to the interaction between metallic parts and metals (Brostow et al., 2006). Also, friction has a dynamic and complex impact on the wear of engineering polymers due to the microscopic and macroscopic surface interactions (Anderson et al., 1996; Amiruddin et al., 2019; Anitha et al., 2001). Therefore, more investigations should be devoted to understanding early and permanent wear and friction processes.

From the insights and discussion in this study, the findings with regard to the running-in application of optimized 3D printing in tribology under various sliding conditions are limited, and recent studies have concentrated on improving the mechanical properties of 3D-printed materials by adjusting the printing parameters. This study on the running-in can improve the tribological

working state dramatically, and can contribute to increased durability with minimum continuous wear, and provide new ideas for the combination of 3D printing with polymer materials. The ability to estimate the expected wear performance (tribological characteristics) of many designs and materials in service is a crucial part of the design processes of bearing mechanisms, plastic rotary components, etc. Therefore, the aim of this study was to analyse the effects of dry running-in stages in relation to the COF and wear rate on an optimized 3D-printed internal triangular flip ABS pin and a 3D-printed solid ABS pin at varying speeds and loads.

2.0 EXPERIMENTAL PROCEDURE

The solid ABS pin and triangular flip ABS pin were modelled using SolidWorks software (Figure 1) and saved in STL (stereolithography) format prior to their fabrication using a FlashForge Creator Pro 3D printer. Meanwhile, a FlashPrint V3.21 slicing software was run to control and fine-tune the printing characteristics. Table 1 shows the optimized 3D-printing parameters that were used for the pin specimens.
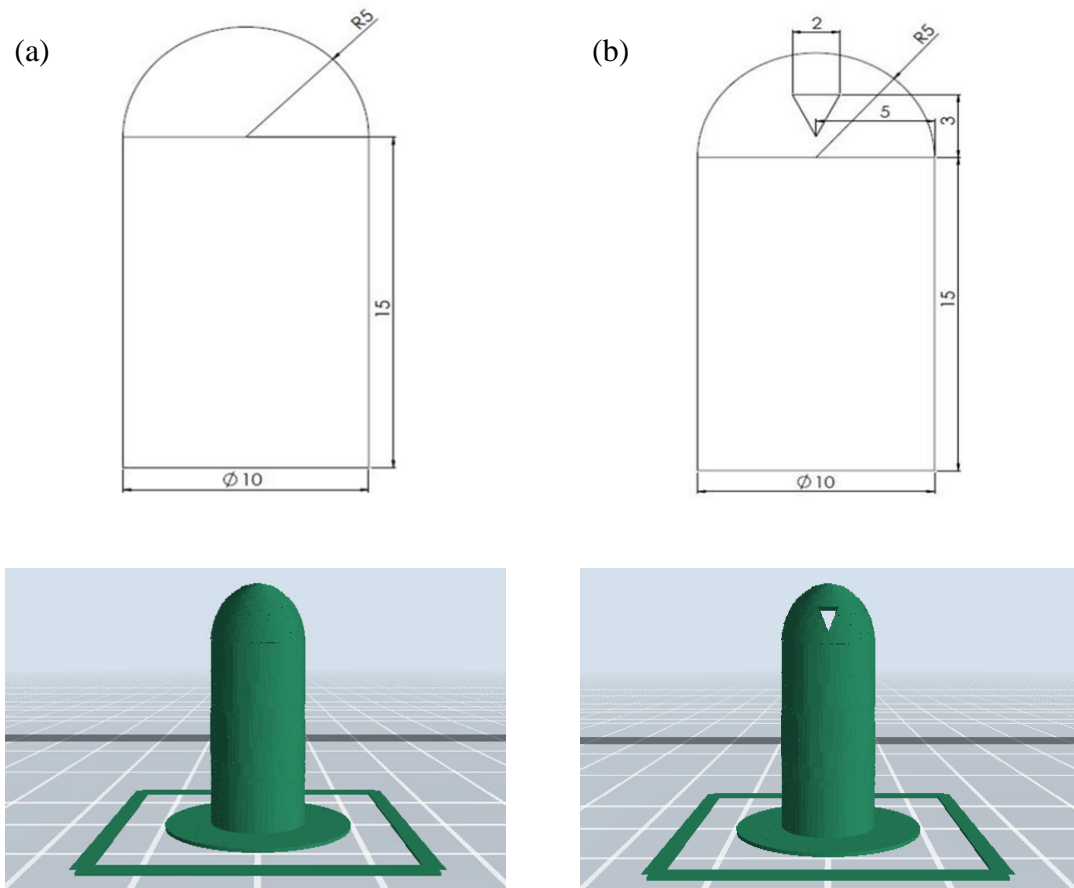

Figure 1: Models used to manufacture the (a) solid, and (b) triangle flip ABS pins. All measurements are in mm.

Table 1: Fixed 3D printing parameters (Norani et al., 2020).

Parameters (unit)	Value
Layer height, H (mm)	0.10
Nozzle temperature, T (ºC)	234
Pattern, P	Triangle
Infill, (%)	100

The ASTM G99-05 tribology test (Standard Test Method for Wear Testing with a Pin-on-Disk Apparatus) was conducted under dry sliding conditions on a pin-on-disc tribometer (Figure 2). Table 2 presents the properties of the pin and disc materials used in the study. These material properties were determined using a compression test (ASTM D695-15, 2015), microhardness test (ASTM E384-17, 2017), and a 3D non-contact profilometer. Both the ABS pins were made to slide against carbon chromium steel. Table 3 illustrates the testing parameters. The pins and discs were cleaned with acetone before the tests were conducted. The COF and specific wear rate (k) were determined using Equations (1) and (2) below:

$$COF = \frac{F}{W} \qquad (1)$$

$$k = \frac{V_{loss}}{WL}; \quad V_{loss} = \frac{m_{loss}}{\rho} \qquad (2)$$

The COF is the ratio of the frictional force (F) to the applied load (W), both of which are measured in Newtons (N). The specific wear rate k [mm³/Nm] was calculated using the loss in volume, V_{loss} [mm³], due to wear and the sliding distance L [m]. m_{loss} denotes the mass loss [g], while ρ represents the density of the material [g/mm³]. The surface morphologies of both ABS pins were inspected under a scanning electron microscope (SEM).
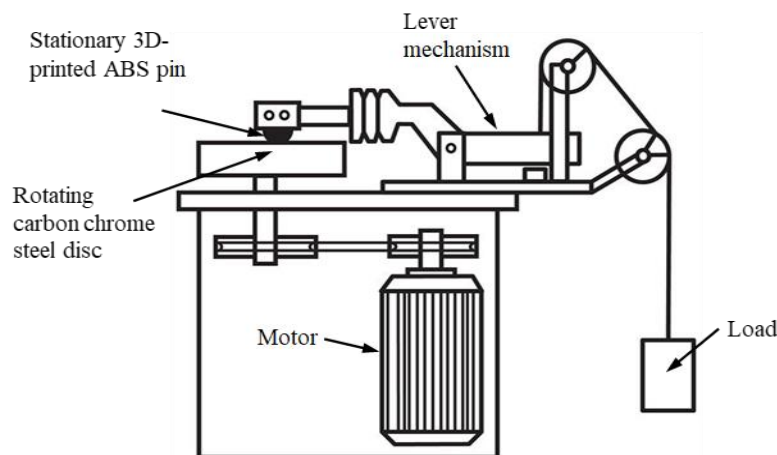

Figure 2: Schematic diagram of a pin-on-disk tribometer.

Table 2: Material properties of all samples prior to testing (Norani et al., 2020).

Material properties	Pins (ABS)	Discs (carbon-chrome-steel)
Hardness (GPa)	0.13	7.45
Young's modulus (GPa)	0.514	210
Density (g/cm^3)	1.07	7.7
Surface roughness (μm)	0.6 - 1.70	0.1 - 0.3

Table 3: Tribology testing parameters.

Parameter	Value
Sliding speed (rpm)	600-800
Sliding distance (m)	1000
Applied load (N)	19.68-58.68
Temperature (^{o}C)	27

3.0 RESULTS AND DISCUSSION

Figures 3 to 5 illustrate the correlation between the COF and running-in distance of both ABS pins at different speeds and loads. It was evident from the break-in maps (Figures 3-5) that changes in the COF occurred at two distinctive stages, namely, the (i) running-in and (ii) steady-state stages. The COF initially increased to its maximum limit before fluctuating in the running-in stage and, after some time, plateauing in the steady-state stage. Therefore, the running-in was affected by the materials in the early stages of sliding.

At a speed of 400 rpm, Figure 3(a) shows that the shortest correlation between the COF and running-in distance for the solid ABS pin was at a loading of 19.62 N, followed by 58.68 N and, lastly, 39.24 N. Figure 3(b) for the triangular flip ABS pin shows that the shortest correlation between the COF and running-in distance was at a loading of 58.68 N, followed by 19.62 N and, lastly, 39.24 N. At a speed of 600 rpm, Figure 4(a) shows that the correlation between the COF and running-in distance for the solid ABS pin was at a loading of 58.68 N, followed by 19.62 N, and finally, 39.24 N. Figure 4(b) illustrates that for the triangular flip ABS pin the shortest correlation between the COF and running-in distance was at a loading of 58.68 N, followed by 39.24 N, and finally, 19.62 N. At a speed of 800 rpm, Figure 5(a) indicates that the correlation between the COF and running-in distance for the solid ABS pin was at a loading of 19.62 N, followed by 58.68N, and lastly, 39.24 N. Apart from that, an increase in the correlation between the COF and running-in distance for the triangular flip ABS pin (Figure 5b) began at 251.466 m (0.325) at a loading of 58.68 N, followed by 649.243 m (0.365) at a loading of 39.24 N, and finally, 691.240 m (0.424) at a loading of 19.62 N. Overall, the general trend of the results corresponded with the findings of Blau (1981), whereby it started with the oxidation segment, followed by plastic deformation, and ended up in the abrasive debris section. The oxidation and abrasive debris parts were significantly related to the ABS because of the oxidative growth of the material, its coarse surface composition, and fluctuations in the surface temperature. Moreover, it was clear that the minimum running-in distance for the solid ABS pin was 196.951 m, and 145.160 m for the triangular flip ABS pin.
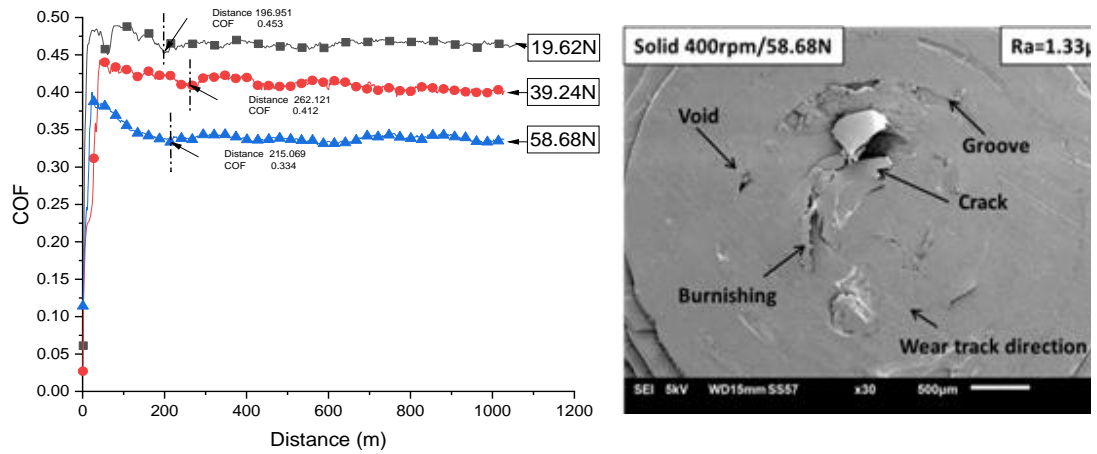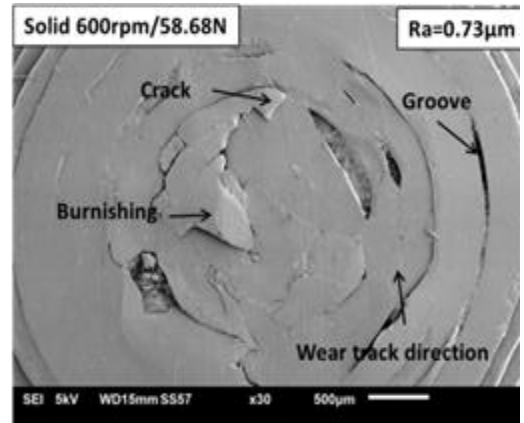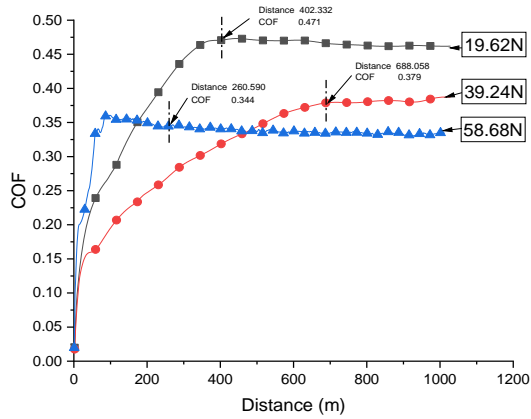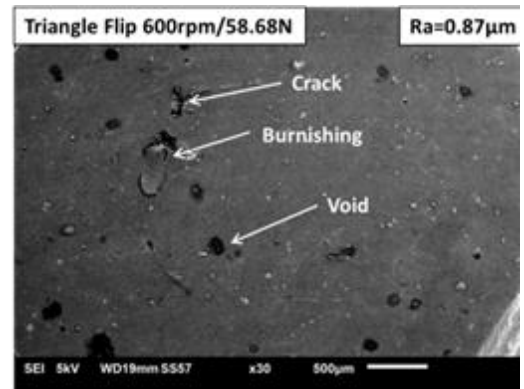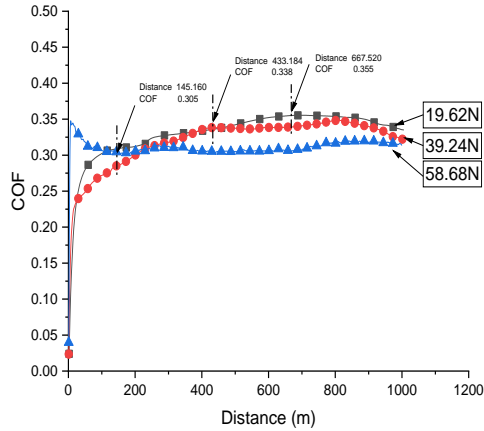
a)
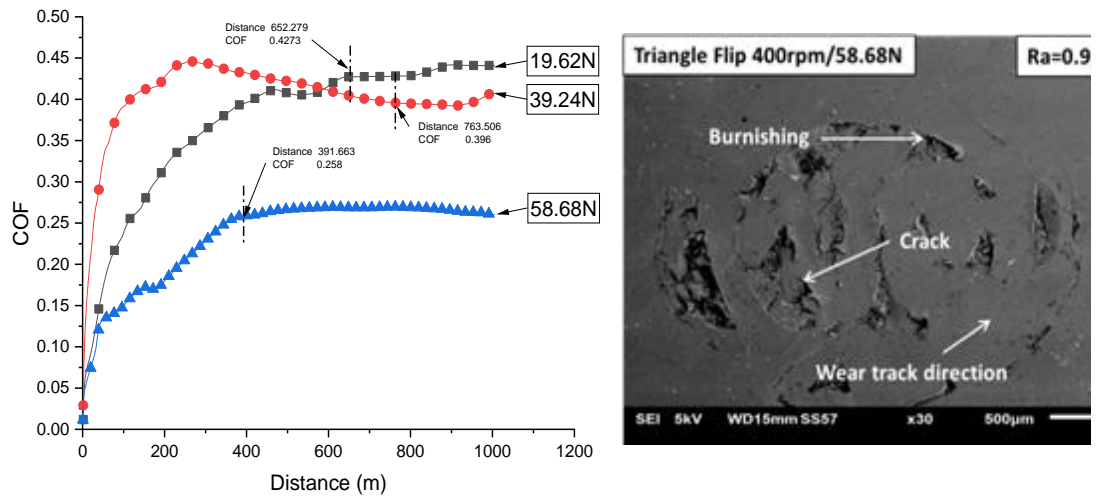
(b)

Figure 3: COF plotted against running-in distance and SEM micrographs of surfaces of 3D-printed (a) solid and (b) triangular flip ABS pins under different loads and at a fixed speed of 400 rpm.
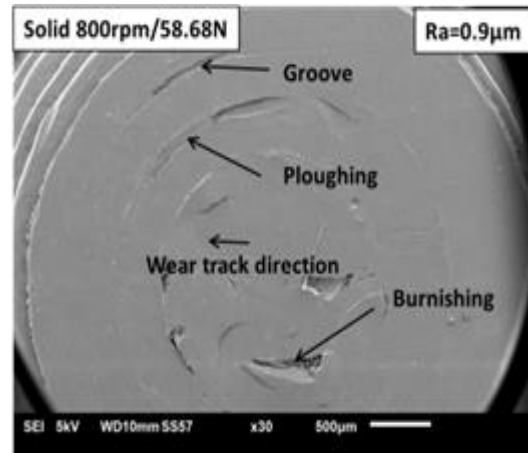
(a)

(b)

Figure 4: COF plotted against running-in distance and SEM micrographs of surfaces of 3D-printed (a) solid and (b) triangular flip ABS pins under different loads and at a fixed speed of 600 rpm.
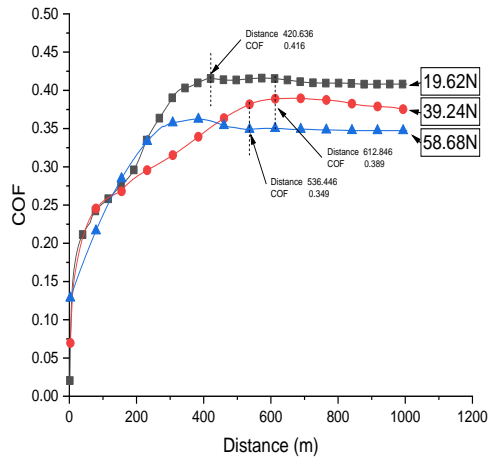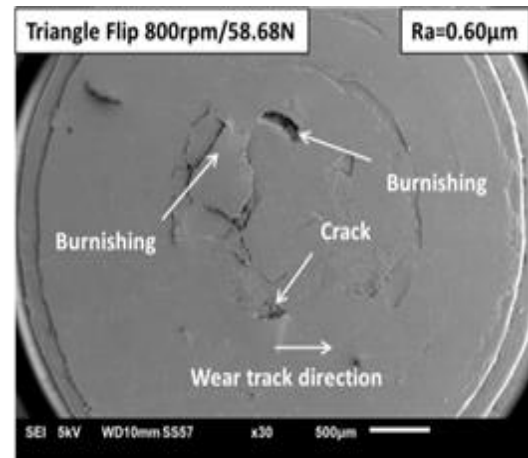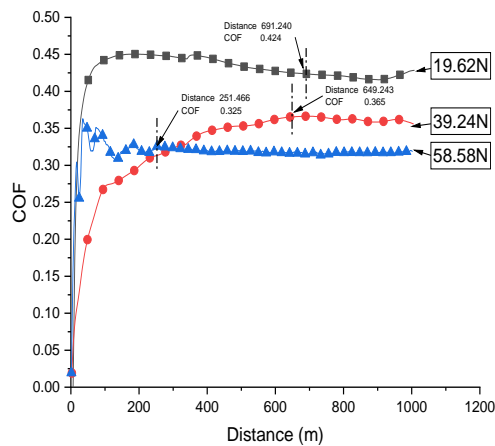
(a)

(b)

Figure 5: COF plotted against running-in distance and SEM micrographs of surfaces of 3D-printed (a) solid and (b) triangular flip ABS pins under different loads and at a fixed speed of 800 rpm.

Figure 6 was derived from the results of the running-in distance and COF in Figures 3 to 5. It shows the correlation between the running-in distance and the steady-state COF of the 3D-printed (a) solid and (b) triangular flip ABS pins under various speeds and loads. According to Figure 6(a), the running-in distance of the solid ABS pin increased as the speed and load were increased, except at a load of 39.24 N. Figure 6(b) displays the fluctuations in the running-in distance of the triangular flip ABS pin, except at a load of 19.62 N. It was observed that the running-in distance required by the triangular flip ABS pin was less than that of the solid ABS pin. This was due to

changes in the surface area composition and microstructural effects earlier in the interaction between the ABS pins and metallic contact disk. Therefore, the earlier steady state in the friction-distance map indicated that there was less power consumption and less sliding resistance (Blau. 1981), and improvements in the early surface interaction under dry sliding conditions.

With regard to the steady-state COF, the COF of both the solid and the triangular flip ABS pins decreased as the load increased at a constant speed. This occurred because the sliding against the metal surface gave rise to two main processes, namely, abrasion and adhesion, to form a thin polymer film. Initially, the process started with abrasion, which loosened the wear particles that been formed and were held within the pins. As the wear continued, the wear particles filled up the surface topology, thereby reducing the abrasion process. Next, adhesion of the thin polymer film occurred and, at same time, another layer of thin film was developed on the pins and the counter face, which, in this case, was the disc surface (Naga et al., 2011). As the adhesion process continued, it resulted in a stable steady-state COF and wear rate.

However, under a fixed load and with variations in the speed, the curve of the steady-state COF exhibited instability. The stable sliding conditions (load, temperature and velocity), roughness pressure, and surface smoothness, which resulted in the formation of a full film track and load carrying area, were variables that affected the COF curve (Blau. 1981; Andersson et al., 1996). In addition, the smooth surface of the 3D-printed pin specimens was more effective in reducing the COF (Amiruddin et al., 2019; Anitha et al., 2001). All these variables were dependent on each other to produce the COF curve.

The triangular flip ABS pin had the lowest COF (0.305) and shortest running distance (145.160 m) at a load of 58.68 N and speed of 600 rpm due to the lower maximum stresses distributed on the contact surface. A low maximum stress will give rise to a low COF in lightweight components, without affecting the strength of the components (Abdollah et al., 2020). Since the thermal conductivity of ABS is lower than that of steel discs, the higher speed and heavier load on the COF caused the pin to deform and decreased the COF. Moreover, the low thermal conductivity generated more heat and better viscoelasticity in the contact zone than the steel disc. These overall findings corresponded with the results obtained by Kumar et al. (2020). With regard to other polymers, PLA, HTPLA and PETG polymers have larger steady-state COFs of 0.55, 0.49 and 0.46, respectively compared to ABS (0.258) at a speed of 400 rpm and load of 58.68 N. On the other hand, the surface orientation of the 3D-printed ABS pins had a significant influence on the friction and wear (Hanon et al., 2020).

The implementation of the triangular flip internal geometry on the inside of the 3D-printed pin specimen affected the stress area concentration at the contact point, thereby decreasing the COF. In other words, the triangular flip internal geometry distributed lower maximum stresses on the contact surface, thereby decreasing the COF deformation which, in turn, prevented wear during the sliding process. Also, Figures 3 to 5 show the SEM micrographs of the surface roughness with the lowest COF being that of the triangular flip ABS pin. Overall, the triangular flip ABS pin had a better surface roughness (0.93~0.60 µm) than that of the solid ABS pin (1.70~0.67µm). The minimum surface roughness of a 3D-printing process reduces the COF as well due to the thickness of the dense layer and the melting temperature of the filament (Kovan et al., 2018). Theoretically, it was observed that the wear rate of the pins was at a minimum when the surface roughness was low.
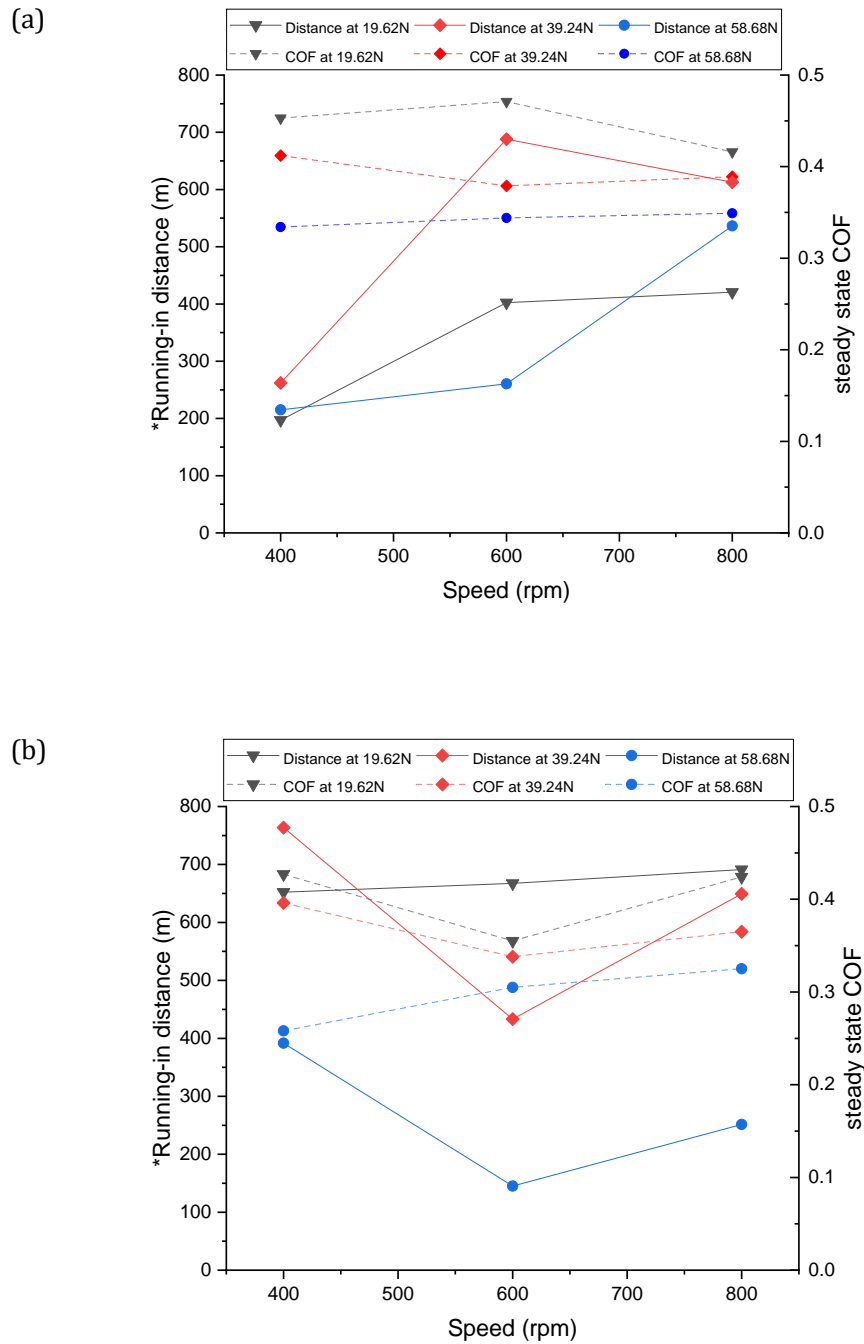
(a)

(b)

Figure 6: COF plotted against running-in distance of 3D-printed (a) solid and (b) triangular flip ABS pins under different loads and speeds.
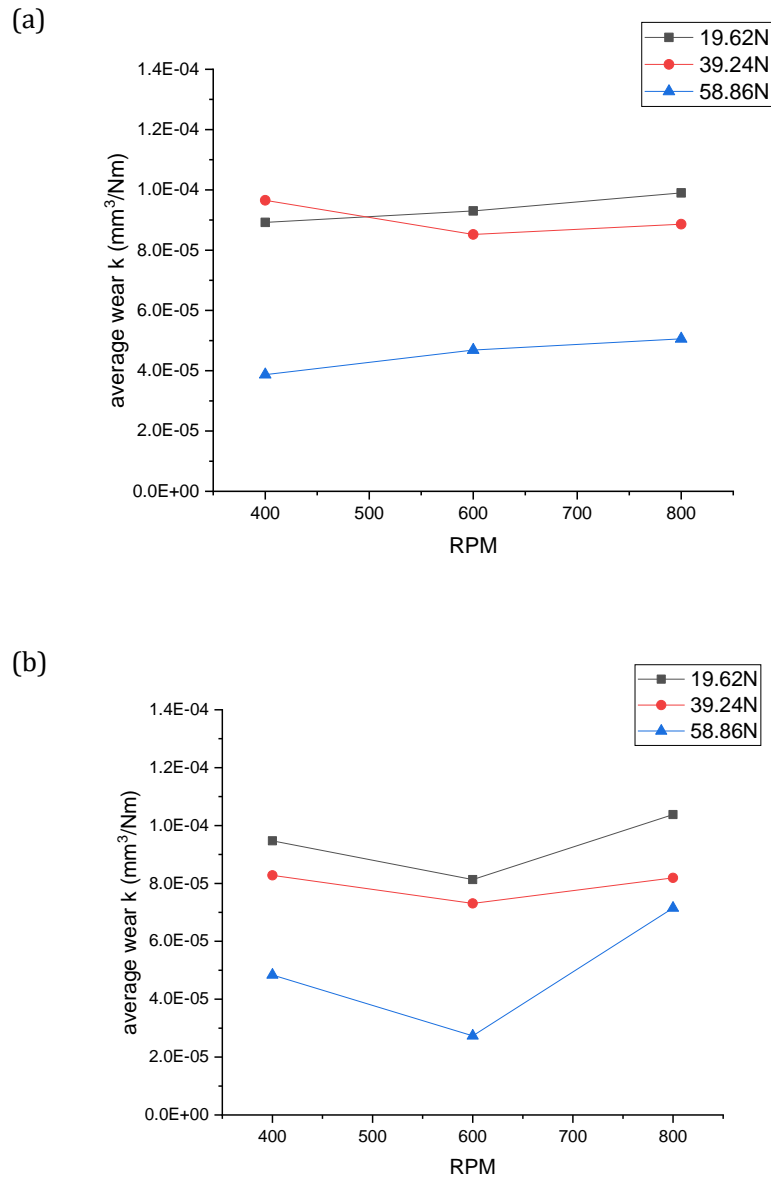
(a)

(b)

Figure 7: Average wear rate of 3D-printed (a) solid and (b) triangular flip ABS pins plotted against changes to applied load and speed.

Figure 7 shows the average wear rate of the 3D-printed ABS pins which determined which load and speed gave the lowest average wear rate. The lowest average wear rate of the triangular flip pin was 2.732 E-5 mm³/Nm, while for the solid pin, it was 3.871 E-5 mm³/Nm. At a specific loading, the average wear rate increased as the applied speed was increased. Logically, the lowest average wear rate will correspond with the longer life and durability of a material. These results were in agreement with the findings of Babat et al. (2013) and Khun et al. (2013) as the pin

specimens exceeded the thermal conductivity of the material and thus, produced more heat at the contact zone as a result of the viscoelasticity of the material (Kumar et al., 2020).

Wear is defined as the negative removal or deformation of the surface of a material. When two surfaces slide across each other, a resistance develops against the motion due to asperity and abrasion. Asperity is defined as the unevenness or roughness of the surface of a material. In the observed surfaces in the SEM micrographs in Figures 3 to 5, the dry sliding process began with the asperities in the form of powder or debris as the load increased. These asperities formed and deformed or sheared the surface of the material due to a difference in the contact (irregular contact). This is known as ploughing. Several volumes of surface materials were detached during the dry sliding process to form abrasive grooves at certain deteriorated points on the surface. With repeated sliding, there was build-up of countless wear particles or the occurrence of plastic flow at the top of the surface. Thus, the surface became smooth and flat, and the asperities became less rigid. As severe wear regimes emerged in the polymer, delamination and burnishing occurred. Layers were removed from the surface of the material due to the high stress levels, and this led to cracking and plastic deformation (Abdollah et al., 2020). Likewise, it was found that the wear rate peaked at the beginning of the process and progressed with higher sliding speeds, regardless of the load. More heat was generated due to wear at the higher speed, whereby the adhered asperities tended to form cracks and grooves, and to delaminate. The cracks that developed on the surface of the material interacted with each other, resulting in the separation and delamination of pieces of the material. The grooves, which had formed as a result of the sliding contact between the smooth surfaces of the ductile materials at the peaks and valleys, were then aligned with the mating surfaces (NCT. 1983; ESDU. 1988). Therefore, the SEM micrograph in Figure 4(b) illustrates the smoothest surface with the least wear mechanism compared to the others.

Increasing the load will flatten the surfaces of the asperities at a constant contact area to subsequently reduce the wear and friction, while increasing the sliding velocity can raise the surface temperature and cause a decrease in the adhesive forces between the contact surfaces (Hatipoglu et al., 2016). As the load increases, the wear resistance will tend to increase as well. The generated wear resistance will cause a rise in the temperature, thereby decreasing the strength of the material and contributing to a rise in friction. The 3D-printed ABS pin correlated with the surface roughness texture and the COF (Amiruddin et al., 2019; Anitha et al., 2001). The smoother the surface, the greater the likelihood that the COF will decrease and recover to a steady-state COF. This is why the pursuit of an increase in the COF is encouraged. It is recommended that chemical or physical measurements of the ABS be made to eliminate ruggedness.

4.0   CONCLUSION

In the present study, the effects during the dry running-in stage of the COF and wear rate on optimized 3D-printed internal triangular flip and solid ABS pins at varying speeds and loads were assessed. The higher the running-in distance, the more power will be required, and the higher will be the sliding resistance, which is not good for certain applications. The findings demonstrated that the 3D-printed triangular flip ABS pin had a significant running-in distance, low steady-state COF and wear rate (145.16m; 0.305) at a loading of 58.68N and a sliding speed of 600 rpm compared to the solid ABS pin. The running-in distance and low steady-state COF were due to the effects of the microstructure of the contact surfaces, changes to the surface composition, the

modulus of elasticity and delamination as well as abrasion to the triangular flip ABS pin. Based on this important note, the 3D-printed internal triangular flip ABS pin gave a better and improved power consumption, smooth sliding resistance and wear surface compared to the solid ABS pin.

REFERENCES
Abdollah. M. F. B., Norani. M. N. M., Abdullah. M. I. H. C., Amiruddin. H., Ramli. F. R., Tamaldin. N. (2020). Synergistic effect of loads and speeds on the dry sliding behaviour of fused filament fabrication 3D-printed acrylonitrile butadiene styrene pins with different internal geometries. The International Journal of Advanced Manufacturing Technology, 1-15.

Amiruddin. H., Abdollah. M.F.B., Norashid. N.A. (2019). Comparative study of the tribological behaviour of 3D-printed and moulded ABS under lubricated condition. Materials Research Express, 6(8), 085328.

Andersson. P., Juhanko. J., Nikkila. A.P., Lintula. P. (1996). Influence of topography on the running-in of water-lubricated silicon carbide journal beatings. Wear, 201, 1-9.

Anitha. R., Arunachalam. S., Radhakrishnan. P. (2001). Critical parameters influencing the quality of prototypes in fused deposition modelling. Journal of Material Processing Technology, 118 (1–3), 385–388.

Babat V, Taşdemir M (2013) Mechanical and wear properties of Acrylonitrile Butadiene Styrene polymer composites. Advanced Materials Research 747:299-302.

Bakar, H. N. A., Ghani, J. A., Haron, C. H. C. (2020). Influence of rounded cutting-edge radius and machining parameters on surface roughness and tool wear in milling AISI H13 steel under dry and cryogenic machining. Jurnal Tribologi, 24, 52-64.

Blau. P. J. (1981). Interpretations of the friction and wear break-in behaviour of metals in sliding contact. Wear, 71, 29-43.

Brostow. W., Chonkaew. W., Menard. K.P. (2006). Connection between dynamic mechanical properties and sliding wear resistance of polymers. Materials Research Innovations, 10(4), 389-393.

ESDU data item 87007. (1988), Design and Material Selection for Dry Rubbing Bearings, Tribology Series, Vol. 8, Engineering Sciences Data Unit International, London.

Franklin. S.E. (2001). Wear experiments with selected engineering polymers and polymer composites under dry reciprocating sliding conditions. Wear, 251, 1591-1598.

Hanon, M. M., Robert, Zsidai. L. (2020). Impact of 3D printing structure on the tribological properties of polymers. Industrial Lubrication and Tribology. 72. 811-818. 10.1108/ILT-05-2019-0189.

Hanon, M.M., Alshammas, Y., Zsidai, L. (2020). Effect of print orientation and bronze existence on tribological and mechanical properties of 3D-printed bronze/PLA composite. Int J Adv Manuf Technol 108, 553–570. doi.org/10.1007/s00170-020-05391-x

Hanon. M.M., Kovács. M., Zsidai. I. (2019). Tribological behaviour comparison of ABS polymer manufactured using turning and 3D printing. International Journal of Engineering and Management Sciences, 4(1), 46-57.

Hatipoglu. G., Kartal. M., Uysal. M., Cetinkaya. T., Akbulut. H. (2016). The effect of sliding speed on the wear behaviour of pulse electro co-deposited Ni/MWCNT nanocomposite coatings. Tribology International, 98, 59-73.

Jasiuk. I., Abueidda. D.W., Kozuch. C., Pang. S., Su. F.Y., McKittrick. J. (2018). An overview on additive manufacturing of polymers. JOM, 70 (3), 275-283.

Khun NW, Liu E (2013) Thermal, mechanical and tribological properties of polycarbonate/acrylonitrile-butadiene-styrene blends. Journal of Polymer Engineering 33(6):535-543.

Kovan. V., Tezel. T., Topal. E.S., Camurlu. H.E. (2018). Printing parameters effect on surface characteristics of 3d printed PLA materials. International scientific journal Machines. Technologies. Materials, 7, 266-269.

Kumar. S., Saha. R., Barnik. (2020). Tribological properties of acrylonitrile butadiene styrene in self-mated contacts and against steel disc. Materials Today: Proceedings. Doi: 10.1016/j.matpr.2020.02.511.

Liu. Z., Wang. Y., Wu. B., Cui. C., Guo. Y., Yan. C. (2019). A critical review of fused deposition modelling 3D printing technology in manufacturing polylactic acid parts. The International Journal of Advanced Manufacturing Technology, 102(9-12), 2877-2889.

Naga Raju B, Ramji K, Prashad V S R K. (2011). Studies on Tribology Properties of Zno Filled Polymer Nanocomposites. Arpn Journal of Engineering and Applied Science. Vol. 6(6). Pp. 75–82.

NCT Polymer Materials for Bearing Surfaces Selection and Performance Guide. (1983) National Centre of Tribology, Risley, Warrington, UK.

Nor MMS, Sudin NM and Razali FM. Application of Taguchi method in investigating the effect of layer thickness and fill angle on FDM parts. IOP Conf Ser Mater Sci Eng 2018; 409: 012018.

Norani, M. N. M., Abdollah, M. F. b., Chua, M. I. H., Amiruddin, H., Ramli, F. Tamaldin, N. (2020). 3D printing parameters of acrylonitrile butadiene styrene polymer for friction and wear analysis using response surface methodology. Proceedings of the Institution of Mechanical Engineers, Part J: Journal of Engineering Tribology. 135065012092560. 10.1177/1350650120925601.

Norani, M.N.M., Abdollah, M.F.B., Abdullah, M.I.H.C., Amiruddin, H., Ramli, F.R. Tamaldin, N. (2020). Correlation of tribo-mechanical properties of internal geometry structures of fused filament fabrication 3D-printed acrylonitrile butadiene styrene. Industrial Lubrication and Tribology. doi.org/10.1108/ILT-04-2020-0143.

Nuruzzaman. D., Chowdhury. M., Rahaman. M. (2011). Effect of duration of rubbing and normal load on friction coefficient for polymer and composite materials. Industrial Lubrication and Tribology, 63, 320-326.

Sabahi, N., Chen, W., Wang, C., Kruzic. J.J., Li. X.A. (2020). A Review on Additive Manufacturing of Shape-Memory Materials for Biomedical Applications. JOM, 72, 1229–1253.

Samira. A., Saghlatoon. H., Honari. M.M., Mirzavand. R., Montemagno. C., Mousa. P. (2018). Investigation on electrical and mechanical properties of 3D printed nylon 6 for RF/microwave electronics applications. Additive Manufacturing 21, 69-75.

Zmitrowicz. A. (2006). Wear patterns and laws to wear a review. Journal of Theoretical and Applied Mechanics, 44(2), 219-253.